Neutron-scattering study of pretransitional dynamics in the deuterated diacetylene monomer 2,4-hexadiynylene bis(*p*-toluenesulfonate)

J. Even, B. Toudic, M. Bertault, and H. Cailleau
Groupe Matière Condensée et Matériaux, URA au CNRS N 804, Université de Rennes I, Campus de Beaulieu, 35042 Rennes Cedex, France

F. Moussa
Laboratoire Léon Brillouin (CEA-CNRS), CE Saclay, 91191 Gif-sur-Yvette Cedex, France
(Received 6 March 1995)

Coherent neutron scattering is used to make a dynamical study of the disubstituted and fully deuterated diacetylene 2,4-hexadiynylene bis(*p*-toluenesulfonate) (*p*TS-D) in the monocrystalline monomer state. The aim of this study is to make a comparison with the dynamics of the same monocrystal in the polymer state [Phys. Rev. B **49**, 11 602 (1994)]. The mechanism leading to the incommensurate phase of *p*TS-D monomer is also discussed. The experimental study shows an overdamped soft mode above T_i. Its evolutions as a function of temperature and its dispersion are described. A central peak related to the presence of defects is also observed. The soft mode presents roughly the same mean-field behavior for *p*TS-D monomer and *p*TS-D polymer. *p*TS-D mixed monomer-polymer crystals are then probably very good prototypes for the study of the influence of pure random field on a structural phase transition.

I. INTRODUCTION

Some disubstituted diacetylene compounds (R—C≡C−C≡C—R', $R=R'$ or $R\neq R'$) present a unique property: they undergo topochemically controlled solid state polymerization in crystalline state.[1] Among them, the most investigated compound is the symmetrical disubstituted diacetylene 2,4-hexadiynylene bis(*p*-toluenesulfonate): it corresponds to $R=R'=CH_3$-C_6H_4-SO_2-O-CH_2 (referred to as *p*TS-H hereafter). In order to perform neutron scattering experiments, we had to make large-size monocrystals of fully deuterated *p*TS-D.[2] Large-size monocrystals of *p*TS-H and *p*TS-D monomers can be converted into single crystals of *p*TS-H and *p*TS-D polymers by exposure to radiation (visible, UV, x, γ) or by thermal annealing. In this last case mixed monomer-polymer crystals of any polymer content can be obtained in a controlled manner. The polymer chains extend along the **b** axis in the monoclinic structure of *p*TS ($P2_1/c$). They are produced homogeneously in the monomer matrix. In other words, in monocrystals with a very low polymer content, polymer chains are distributed at random. These first polymer chains contain around 20 monomer units.[3]

The second interesting property of *p*TS is that structural phase transitions occur both in the monomer and polymer crystals. *p*TS monomer and polymer are isomorphous at room temperature.[4–9] The transitions are associated with librational motions of the polar side groups, yielding a doubling of the unit cell along the *a* crystallographic axis and two inequivalent sites for each structural unit. *p*TS monomer and polymer are isomorphous also at low temperature.

In the case of a *p*TS-H monomer, an intermediate incommensurate phase was discovered.[3] The modulation extends along the *b* axis. This modulated phase is observed in *p*TS-H up to 10% of polymer content.[10] The structural instabilities of *p*TS-H monomer have also been studied by neutron diffraction,[11,12] differential scanning calorimetry,[13,14] and dielectric measurements.[15] The dynamics of the phase transitions of *p*TS monomer has not been so accurately described. A Raman study performed on a *p*TS monomer crystal indicated the existence of a soft mode over a large temperature range from 9 K to T_i.[16] The authors, however, pointed out that the clearly displacive regime observed was in disagreement with the study of thermal motions analyzed by x-ray diffraction,[7] which merely shows an intermediate regime between order-disorder and displacive. The contradiction also appeared in the preliminary results of neutron inelastic scattering experiments.[11] On the other hand, the pretransitional dynamics in *p*TS-D polymer has been described:[8] a soft mode is observed above and below T_c by neutron and Raman scattering. The soft mode becomes overdamped at $T\approx T_c+50$ K ($T_c=182$ K). In addition, the growth of a central peak is clearly observed above T_c. This central peak is attributed to defects, probably related to incomplete polymerization.

The aim of this work was first to make a comparison between the pretransitional dynamics of *p*TS-D polymer and *p*TS-D monomer, second, to try to give some informations about the origin of incommensurability, and third, to determine physical quantities (dispersions, etc. . .) for the study of the incommensurate phase.[17] We must also point out that to know this information is interesting for the study of mixed monomer-polymer crystals which is now in progress.

Preliminary results were presented in Ref. 18. In this work experimental methods are described in Sec. II. In Sec. III the behavior of the soft mode as a function of

0163-1829/95/52(10)/7142(9)/$06.00

temperature is presented. In Sec. IV dispersion curves are studied. The last section is devoted to the discussion.

II. EXPERIMENTAL DETAILS

A. Crystal growth

We used a large-size single crystal of fully deuterated *p*TS-D for the inelastic coherent neutron scattering experiment. *p*TS-D was synthesized and purified according to Ref. 2. The 0.5 cm^3 sample was grown by a slow evaporation (7 days at +4 °C) of an acetone solution. It was already darker red than the color of much smaller size monocrystals which appear rather pink after a faster growth. We think that this fact may explain the small polymer content measured during our neutron scattering experiments: $X=1.5\pm0.5\%$. The short exposition of the sample (a few hours) to room temperature before each experiment did not produce any significant polymerization. Indeed no reduction of b parameter was observed. The sample was kept 18 days at −18 °C and 10 h at 25 °C before the first experiment, 104 days at −18 °C and 18 h at 25 °C before the second experiment. The b parameter was measured in both cases as a function of temperature [Fig. 1(a)] giving the same polymer content. Indeed the b parameter evolution as a function of polymer content is known to be very steep for $X\leq75\%$.[3,19] It is in good agreement with the study of isothermal polymerization kinetics for *P*TS-H as a function of temperature,[20] which shows a very slow polymerization at $T\leq50$ °C. Neutron by themselves do not induce polymerization but it is known that γ rays can induce the polymerization of diacetylenes. In our case no interaction of the sample with the neutron flux was observed. Indeed this result is confirmed in Ref. 21 where no evolution of polymer content through the monitoring of the b value was measured. The initial polymer content ($X=1.5\pm0.5\%$) is determined by comparison of the b value in our *p*TS-D sample at $T=280$ K ($b\simeq5.157$ Å) to the b value given by Ref. 11 at $T=280$ K in *p*TS-D powder where it was measured as a function of polymer content X. It should be noted that it is much easier to obtain a small X value for powder than for monocrystals grown in solution.[20]

B. Neutron scattering

Inelastic neutron scattering has been performed on a three-axis spectrometer 4*F*1 using a cold-neutron source at the reactor Orphée (Laboratoire Léon Brillouin, Saclay). The incident neutron wave vector was held fixed at $k_I=1.4$ Å^{-1} ($E_I=4$ meV) except for a spectrum at $T=221.6$ K, where $k_I=1.64$ Å^{-1}. The width in energy of the resolution function was 30 GHz for vanadium. A beryllium filter cooled with liquid nitrogen was used to remove high-order neutrons from the beam. The sample was mounted on a Displex close-cycle refrigerator installed on the sample table and ensuring a temperature stability less than 0.1 K. The scattering plane was chosen (a^*,b^*) because b is the direction of incommensurability and a is the cell-doubling axis of the low-temperature phase. The critical wave vector $\mathbf{q}_S=\frac{1}{2}a^*+\delta b^*$, where δ is the incommensurability parameter ($\delta\approx0.06$ above $T_i=195$ K[9]). Constant $\mathbf{Q}$ scans were performed in order to record inelastic neutron scattering spectra. The refinements of the neutron data were performed at the Laboratoire Léon Brillouin with their fitting procedures.[22] The soft mode frequency and damping constants were obtained from a damped harmonic oscillator function

$$S(\mathbf{Q},\omega)=\frac{\omega\Gamma|F(\mathbf{Q})|^2}{\left[1-e^{-\hbar\omega/k_BT}\right]\{[\omega^2-\omega_c^2(\mathbf{q})]^2+\omega^2\Gamma^2\}},$$

where $\omega_c(\mathbf{q})$ is the frequency of the mode propagating with the vector $\mathbf{q}$ originating from the critical point of the reciprocal space $\mathbf{Q}_S=\mathbf{q}_S+\mathbf{G}_{hkl}$. Γ is the damping constant and $F(\mathbf{Q})$ the dynamic structure factor. This scattering function is convoluted by the spectrometer response function in order to get the measured intensity.

C. Preliminary measurements

Figure 1(a) shows the evolution of the b parameter as a function of temperature for our *p*TS-D monomer crystal. It is then possible to calculate the thermal expansion coefficient along the b axis: it is equal to 101×10^{-6} K^{-1}.

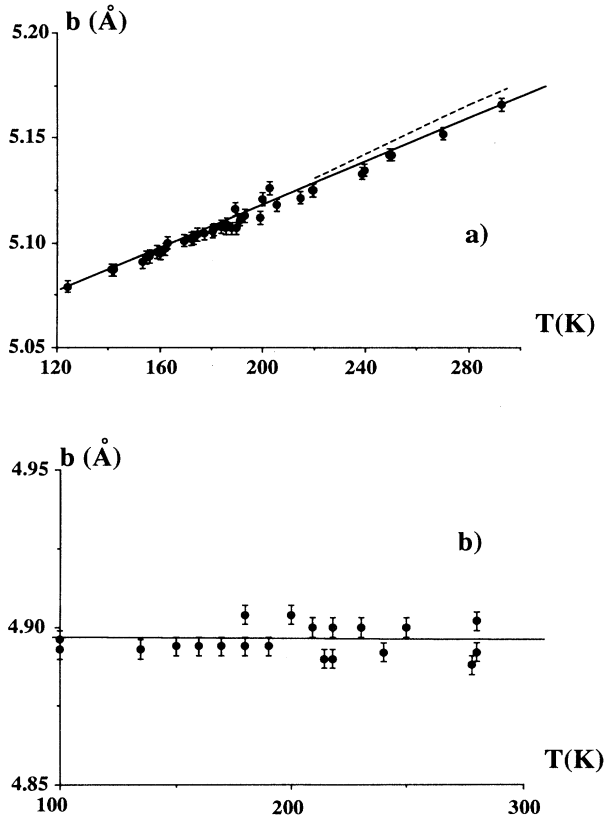

FIG. 1. (a) Evolution of the b parameter for *p*TS-D monomer as a function of temperature. Dashed line represents the evolution as a function of temperature of the b parameter in a *p*TS-D monomer powder.[28] (b) Evolution of the b parameter for *p*TS-D polymer as a function of temperature.

The value found in Ref. 11 for pure monomer pTS-D powder is 114×10^{-6} K^{-1}. The slightly smaller value measured in our crystal confirms the fact that it has a small polymer content. Figure 1(b) shows the evolution of the b parameter as a function of temperature for our crystal but in the fully polymerized state.[9] No thermal expansion is detected in agreement with Ref. 11. This is explained by the substitution of van der Waals bonds by covalent bonds along the polymerization axis b. Indeed in our case at $T=280$ K the b parameter is reduced by 5% between the monomer and the polymer. This very important reduction does not, however, increase the intermolecular contacts between side groups along the b axis because in pTS-D monomer the packing along b is determined only by the positions of the diacetylene back bones.[7]

The situation is different along the a axis [Fig. 2(a)]. In this case there is almost no thermal expansion and maybe even a small negative slope below T_i. These results are similar to ones obtained in Ref. 11 for a pTS-H monomer crystal. This could be explained by the numerous contacts existing along the a axis between neighboring side groups and diacetylene back bones.[7] Figure 2(b) shows the evolution of the a parameter as a function of temperature for the same crystal in the fully polymerized state.[9] Again an anomaly is detected around the critical temperature. In both cases the anomalous behavior of the a parameter indicates that steric interactions along the a axis

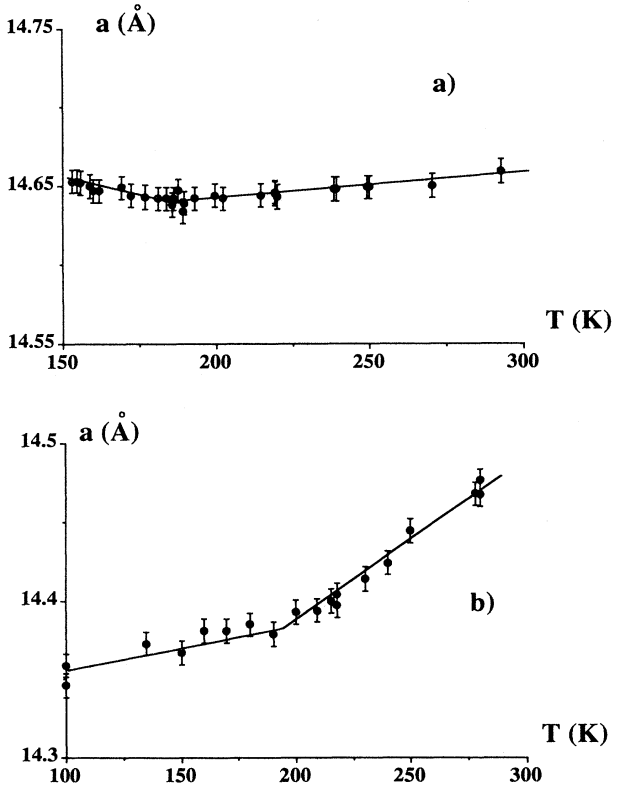

FIG. 2. (a) Evolution of the a parameter for pTS-D monomer as a function of temperature. (b) Evolution of the a parameter for pTS-D polymer as a function of temperature.

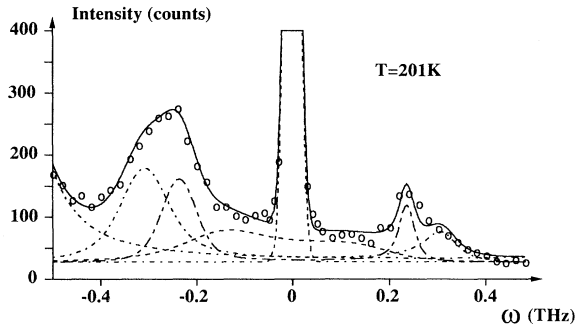

FIG. 3. Inelastic neutron scattering spectrum of pTS-D monomer crystal at $T=201$ K measured at $Q_s-0.25a^*$ point of the reciprocal space [$\mathbf{Q}=(3.25,0.945,0)$]. The acoustic modes appear narrower on the right side (positive energy transfer) than on the left side (negative energy transfer).

may play a role in the structural instability.

In the case of a pTS monomer, the critical wave vector ($\mathbf{q}_S=a^*/2\pm\delta b^*$) lies near the zone boundary, but we must take into account low-frequency acoustic phonons when studying the dispersion along the a axis. Figure 3 shows an example of the spectra obtained when coming closer to the zone center $\mathbf{Q}_s-0.25a^*$. The first contribution is the overdamped soft mode located around $\omega=0$. The second and third contributions are attributed to two acoustic phonons originating from the zone center. We must note that the acoustic modes appear narrower on the right side (positive energy transfer) than on the left side. The focusing is a well-known effect of the three-axis spectrometer resolution function;[23] it is taken into account by the fitting computer program.

III. DYNAMICS IN THE HIGH-TEMPERATURE PHASE: TEMPERATURE DEPENDENCE

A. Soft mode

Inelastic spectra were recorded at the (2.5; 1±δ; 0) or (3.5; 1±δ; 0) point of the reciprocal space. The value of δ was set to the maximum of the diffuse scattering measured during the elastic study.[9,18] Figure 4 shows the evolution of the inelastic spectra from $T=273$ K to $T=214$ K. No inelastic spectra were recorded at temperatures higher than $T=273$ K to prevent polymerization to occur during experiment. The counting time for the spectrum at $T=273$ K is already 16 h. A low-frequency mode is observed at $T=273$ K with $\omega_c=0.25$ THz and $\Gamma=0.38$ THz. For temperatures below $T=273$ K, the soft mode appears overdamped (the damping of the soft mode $\Gamma(q)$ as a function of q was held constant, neglecting the q dependence of $\Gamma(q)$ in the neighborhood of $\mathbf{Q}_S$). In this case, when $\omega_c(q)\ll\Gamma$, the scattering cross section of the soft mode is reduced to $S(q,\omega)=1/\tau_q/(\omega^2+1/\tau_q^2)$ with $1/\tau_q=\omega_c^2(q)/\Gamma$. In other words, it means that the scattering cross section can be described by one parameter ($1/\tau_q$) rather than two parameters [$\omega_c(q),\Gamma$]. Some constraints must then be imposed in the fitting procedure to avoid a correlation be-

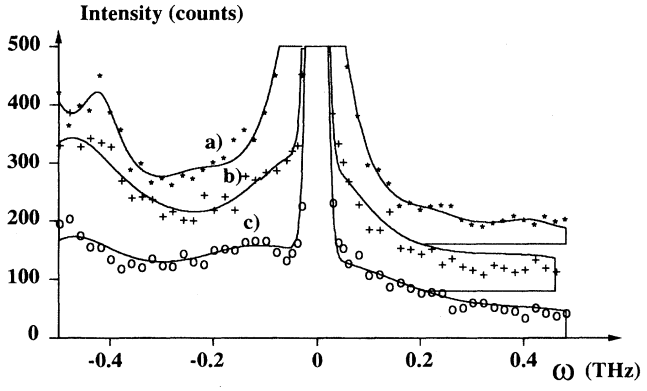

FIG. 4. Inelastic neutron scattering spectra of pTS-D monomer measured at $\mathbf{Q}_S$: (a) $T=214$ K, (b) $T=239$ K, (c) $T=273$ K.

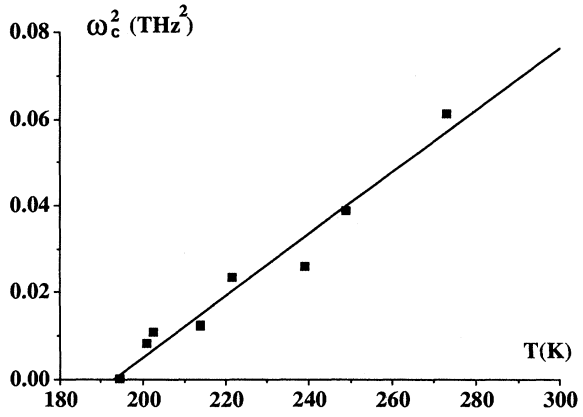

FIG. 6. Temperature dependence of frequency square of the soft mode.

tween $\omega_c(q)$ and Γ. One possibility is to fix the dynamic structure factor $F(\mathbf{Q})$. But this possibility has, in our case, two drawbacks: first, δ is varying as a function of temperature; second, the spectra were recorded at two different points making the comparison more difficult. We used another possibility as for K_2SeO_4:[24,25] to choose an intermediate value between the damping constant for the soft mode above T_i and the damping constant for the amplitude mode below T_i measured by Raman scattering. In the case of a pTS-D monomer, a similar method is used. Figure 5 shows the evolution of the soft mode damping as a function of temperature. It provides a reasonable estimate between the value for the amplitudon mode measured by Raman scattering in the incommensurate phase[9] and the value for the underdamped soft mode at $T=273$ K (Fig. 5). In Ref. 18 preliminary neutron scattering results for the overdamped soft mode were fitted using the approximate expression $S(q,\omega)\approx 1/\tau_q/(\omega^2+1/\tau_q^2)$ but more precise information (Raman scattering) about the damping was lacking.

Figure 6 shows that the soft mode in mono-pTS-D has a mean-field behavior in agreement with the following expression: $\omega_c^2(q=0)=a(T-T_i)$ where $T_i=193$ K and $a=7.1\times10^{-4}$ THz^{2}K^{-1}. This value ($T_i=193$ K) is in good agreement with the value ($T_i=195$ K) obtained from the static study.[9] The ω_c value at $T=195$ K was obtained by measuring the value at $\mathbf{Q}_S-0.2a^*$ and by extrapolating the value at $\mathbf{Q}_S$ using the dispersion along a^* determined at $T=201$ K (see Sec. IV B). A direct determination at $\mathbf{Q}_S+$ and at $T=195$ K would not have been possible.

B. Central peak

The analysis of our spectra was performed by also adding to the damped harmonic oscillator function of the soft mode, an elastic $\delta(\omega)$ component which increases near T_i (Fig. 7). The elastic $\delta(\omega)$ component is equal to the sum of elastic incoherent scattering and central peak contributions. The incoherent elastic scattering, which is

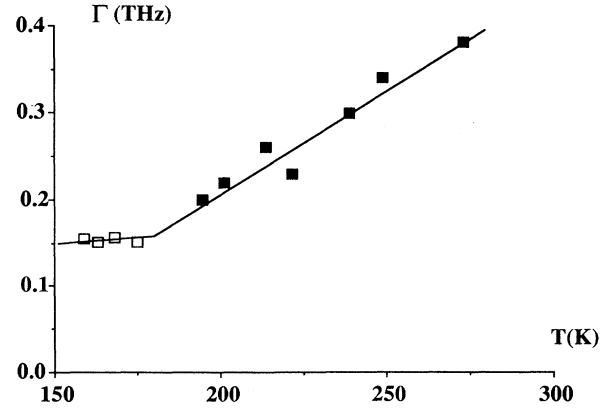

FIG. 5. Evolution of the soft mode damping as a function of temperature. The value below $T=175$ K (open square) are obtained by Raman scattering.[17]

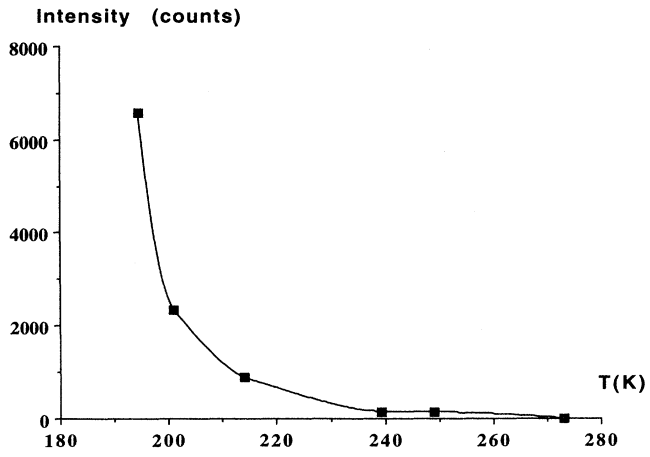

FIG. 7. Evolution of the central peak intensity as a function of temperature. The value at $T=195$ K is obtained by assuming that the central peak dispersion at $T=201$ K remains valid at $T=195$ K.

weakly temperature and Q dependent, was measured far away from Q_S. The elastic peak at $T=273$ K contains almost only elastic incoherent scattering. The observed value of the central peak intensity at $T=195$ K was obtained by assuming that the central peak dispersion at $T=201$ K (Sec. IV C) remains valid at $T=195$ K for $Q_S-0.2a^*$. We must point out that the temperature dependence of the central peak probably indicates that the soft mode structure factor also has a temperature dependence because the central peak and the soft mode are parts of the order parameter fluctuation spectrum.[8]

IV. DYNAMICAL STUDY IN THE HIGH-TEMPERATURE PHASE: q DEPENDENCE

A. Acoustic modes

The plotting of phonon dispersion curves can be obtained from inelastic neutron scattering study. Figures 8 and 9 describe the evolution of the phonon dispersions along the a^* axis at $T=201$ K and $T=249$ K. As previously indicated (Sec. II C), one must take into account the acoustic modes propagating along the a^* axis and originating from the Brillouin zone center. Different contributions are present on the energy scan for 8(d) and 9(c). The first contribution is the overdamped soft mode located around $\omega=0$. The second and third contributions are attributed to two acoustic phonons. The lowest frequency acoustic mode is the TA1 mode which is polarized along b.[26,27] The TA2 and LA are polarized in the (a,c) plane. Thus the three acoustic modes can be measured around $\mathbf{Q}_S=(3.5,0.945,0)$ (Figs. 8–11) or $\mathbf{Q}_S=(2.5,0.94,0)$ (Figs. 9 and 10).

It is necessary here to make a brief review of the measured sound velocities found in the literature. Table I shows the values found by different authors together with our own results. It must be pointed out that some discrepancies exist between Brillouin scattering[26] and ultrasonic measurements[27] performed on pTS-H. Some

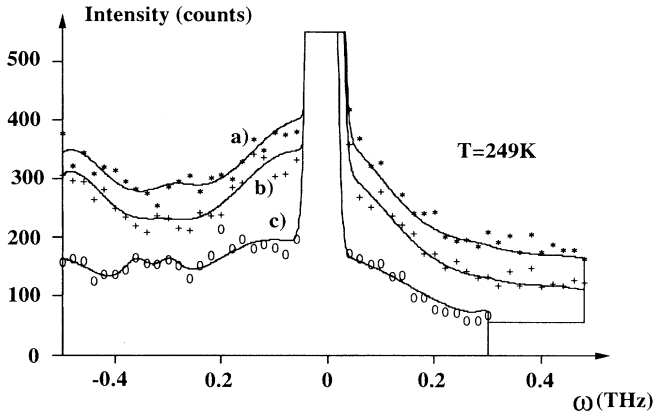

FIG. 9. Evolution of the inelastic neutron scattering at $T=249$ K along the a^* direction: (a) $\mathbf{Q}_S$, (b) $\mathbf{Q}_S+0.08a^*$, (c) $\mathbf{Q}_S-0.20a^*$ [$\mathbf{Q}_S=(2.5, 0.94,0)$].

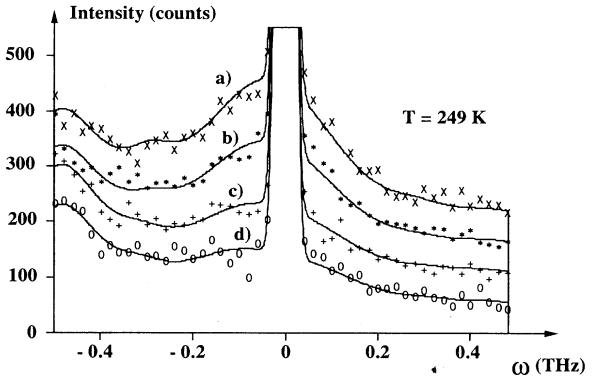

FIG. 10. Evolution of the inelastic neutron scattering spectra at $T=249$ K along the b^* direction: (a) $\mathbf{Q}_S$, (b) $\mathbf{Q}_S-0.011b^*$, (c) $\mathbf{Q}_S-0.026b^*$, (d) $\mathbf{Q}_S-0.036b^*$ [$Q_s=(2.5,0.94,0)$].

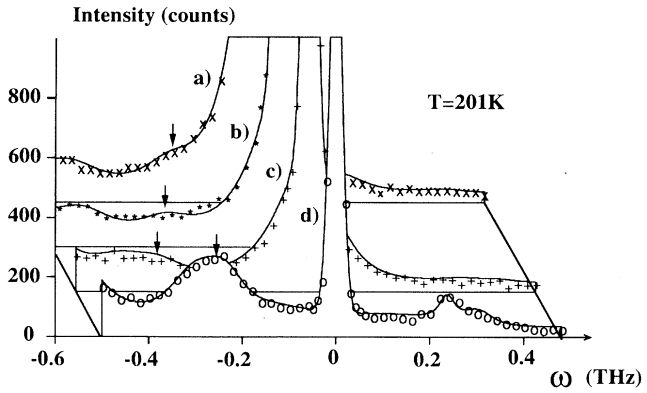

FIG. 8. Evolution of the inelastic neutron scattering spectra at $T=201$ K along the a^* direction: (a) $\mathbf{Q}_S$, (b) $\mathbf{Q}_S-0.05a^*$, (c) $\mathbf{Q}_S-0.10a^*$, (d) $\mathbf{Q}_S-0.25a^*$. The arrows indicate the existence of a weak phonon contribution which is attributed to TA_2 [$\mathbf{Q}_S=(3.5,0.945, 0)$].

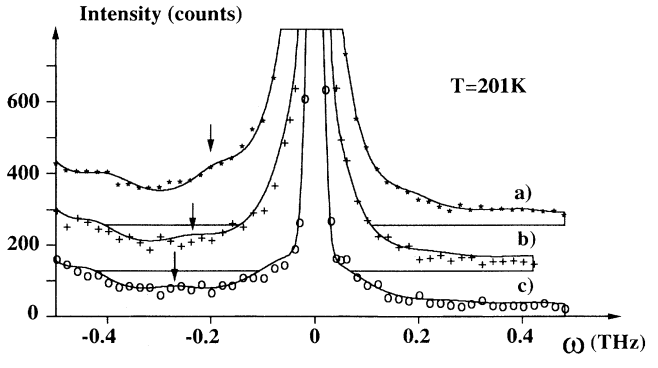

FIG. 11. Evolution of the inelastic neutron scattering spectra at $T=201$ K along the b^* direction: (a) $\mathbf{Q}_S$, (b) $\mathbf{Q}_S-0.020b^*$, (c) $\mathbf{Q}_S-0.045b^*$. The arrows indicate the existence of a weak phonon contribution which is attributed to TA_2 [$\mathbf{Q}_S=(3.5, 0.945, 0)$].

TABLE I. Sound velocities of acoustic phonons propagating along a^* in pTS-H and pTS-D monomer crystals.

	Ref. [26] $T=293$ K pTS-H	Ref. [27] $T=250$ K pTS-H	Ref. [28] $T=240$ K pTS-D
TA1	1040 ms^{-1}	850 ms^{-1}	1140 ms^{-1}
TA2	1560 ms^{-1}	1170 ms^{-1}	1290 ms^{-1}
LA	2490 ms^{-1}	2150 ms^{-1}	
	This work $T=249$ K pTS-D	This work $T=201$ K pTS-D	
TA2	1280 ms^{-1}	1230 ms^{-1}	
LA	1580 ms^{-1}	1620 ms^{-1}	

unpublished results obtained on pTS-D[28] are also reported in Table I. The mean value for TA1 and TA2 sound velocities in literature are then 1010 and 1340 ms^{-1}. Our first acoustic contribution corresponding to a sound velocity equal to 1280 ms^{-1} at $T=249$ K is probably the TA2 mode. The second contribution should then be the LA mode. Our experimental sound velocity (1580 ms^{-1} at $T=249$ K) is around 30% smaller than the values found by Brillouin scattering[26] and ultrasonic measurements.[27] One must, however, keep in mind that Brillouin scattering and ultrasonic measurements are performed at very low q values (near the zone center). Finally we must point out that our group theory analysis (Sec. V A) shows that the TA1 mode corresponds to the soft phonon branch.

B. Soft mode

The study of the soft mode's dispersions along the a^* and b^* axes gives information about the anisotropy of the associated correlation lengths ξ_a and ξ_b. $\omega_c^2(q)$ was fitted to a dispersion law $\omega_c^2(q)=\omega_c^2(0)+\alpha_a q_a^2+\alpha_b q_b^2$, where q_a and q_b are defined by the relation $\mathbf{q}=q_a a^*/a^* + q_b b^*/b^*$. The damping of the soft mode $\Gamma(q)$ was held constant, neglecting the $\mathbf{q}$ dependence of $\Gamma(q)$ in the neighborhood of Q_S (Sec. III A). The same procedure was used for the overdamped soft mode phason of K_2SeO_4.[24,25]

Figure 10 shows the dispersion along the b^* axis at $T=249$ K. The soft mode remains overdamped far from the satellite. Taking into account the results obtained along a^* (Fig. 9) and b^* (Fig. 10) [$\Gamma=0.34$ THz], we found $\alpha_a=1.6$ THz^2 Å^2 and $\alpha_b=4.1$ THz^2 Å^2. The anisotropy ξ_b/ξ_a is equal to the square root of α_b/α_a:[29] $\xi_b/\xi_a \cong 1.6$. This anisotropy is also determined at $T=201$ K.

Figure 11 shows the evolution of inelastic neutron-scattering spectra at $T=201$ K along the b^* direction. The overdamped soft mode is softening near Q_S, together with an additional weak phonon indicated by an arrow. In Fig. 8 (dispersion along the a^* direction) the same phenomenon is observed. The soft mode dispersion coefficients α_a and α_b can be determined: $\alpha_a=2$ THz^2 Å^2 and $\alpha_b=3$ THz^2 Å^2 [$\Gamma(q)=0.22$ THz]. The

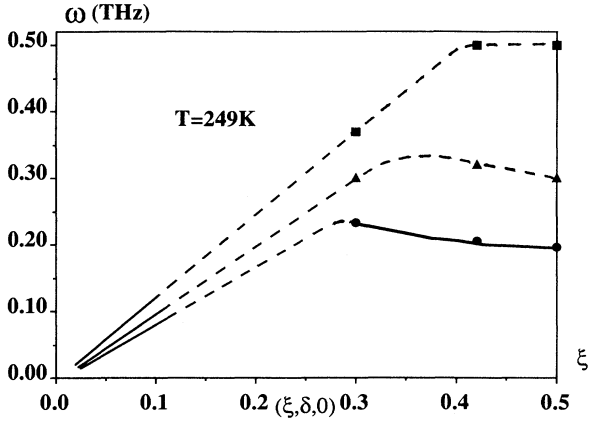

FIG. 12. Dispersion curves along a^* at $T=249$ K for the soft mode (TA_1), the TA_2, and LA acoustic modes. Dashed lines between experimental points correspond to our interpretations of the correlations between modes at different points of reciprocal space.

anisotropy is weak: $\xi_b/\xi_a=\sqrt{\alpha_b/\alpha_a}=1.2$ and $\xi_b=\sqrt{\alpha_b/\omega_c^2}=19$ Å, $\xi_a=\sqrt{\alpha_a/\omega_c^2}=16$ Å. Figure 12 gathers all the results from the study of the dispersion curves along a^* at $T=249$ K and Fig. 13 at $T=201$ K, with our interpretations (Secs. IV A and V A). Our results indicate that a two-dimensional character of the phase transition involving the (a^*,c^*) plane does not provide a good description of the phase transition in the pTS-D monomer as in the case of the pTS-D polymer[8] because ξ_b/ξ_a are similar in both cases.

C. Central peak

The evolution of the central peak intensity at $T=201$ K along a^* and b^* is plotted in Figs. 14(a) and 14(b). We have first assumed that it corresponds to a simple Lorentzian function according to a Landau description [Fig. 14(a)]:

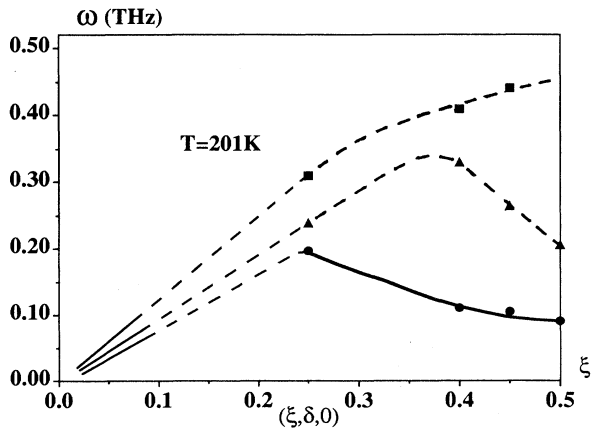

FIG. 13. Dispersion curves along a^* at $T=201$ K for the soft mode (TA1), the TA2 and LA acoustic modes. Dashed lines between experimental points correspond to our interpretations of the correlations between modes at different points of reciprocal space.

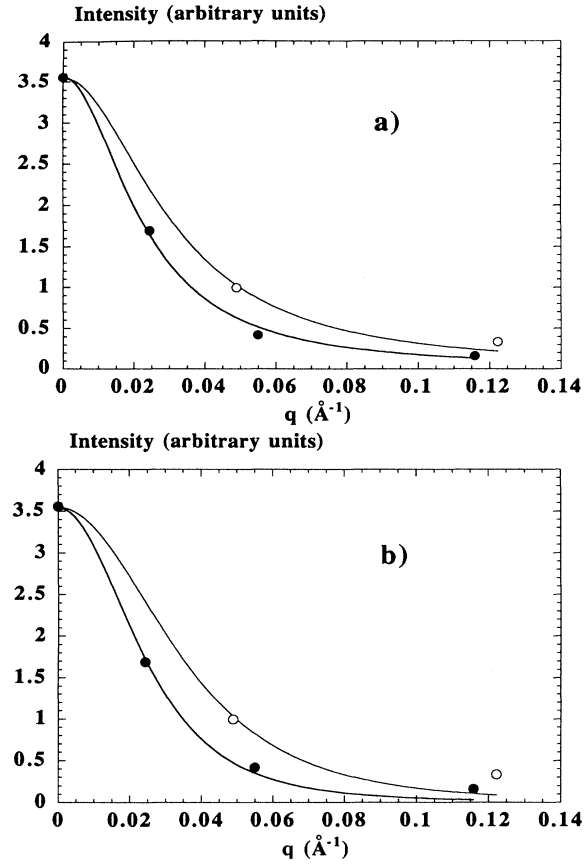

FIG. 14. Evolution of the central peak intensity along the a^* and the b^* directions at $T=201$ K: (a) assuming a simple Lorentzian shape or (b) a square Lorentzian shape.

$$S(\mathbf{Q})\alpha\frac{1}{(1+q_a^2L_a^{-2}+q_b^2L_b^{-2})} .$$

L_a is then equal to 32±3 Å and L_b to 44±3 Å. It must be pointed out that the half width at half maximum of the resolution function is much smaller than $1/L_a$ or $1/L_b$. L_a and L_b are much larger than ξ_a and ξ_b: the soft mode (ξ) and central peak (L) correlation lengths have different physical meaning if $S(\mathbf{Q})$ is described by a simple Lorentzian function.

The Landau theory on the influence of defects on structural phase transitions[30,31] shows that the study of the q dependence of the central peak intensity may be related to ξ_a and ξ_b. For nonferroelectric and nonferroelastic phase transitions and in the simplest case of defect, the scattering intensity corresponding to the central peak is not a simple Lorentzian function but a square Lorentzian function:

$$S(\mathbf{Q})\alpha\frac{1}{(1+q_a^2\xi_a^{-2}+q_b^2\xi_b^{-2})^2} .$$

The fits of central peak intensity with this function [Fig. 14(b)] yield the values of ξ_a and ξ_b: $\xi_a=19\pm2$ Å and $\xi_b=27\pm2$ Å. These values are 20–30% larger than the values of ξ_a and ξ_b found by a direct study of the soft mode (Sec. IV B). It should be stressed that this discrepancy is not so large if one takes into account the experimental difficulty in separating the contributions of the central peak and soft mode (Figs. 8 and 11). The central peak can, however, be definitively attributed to defects because its intensity increases in samples containing a higher polymer content.[9] The Landau theory[31] also predicts that the crossover temperature T_c at which the two elastic contributions (soft mode and central peak) are equal, is given by $(T-T_i)/T_i$ of the order of 10^{-1} (for a defect concentration of the order of 10^{-2}). In our case this crossover should be located a few ten degrees above $T_i=195$ K. It may then explain why the central peak contribution can be measured at $T=201$ K and not at $T=249$ K. So a higher polymer content should make the study of the q dependence of the central peak easier. This study is in progress.

V. DISCUSSION

A. Incommensurability

pTS belongs to type-II incommensurate systems which do not possess a Lifschitz invariant.[32] Thiourea and $NaNO_2$ are among the most well-known compounds of these types of systems.[33,34] In these typical systems the structural phase transition is related to a one-dimensional zone-center irreducible representation. pTS monomer presents a slightly different behavior: the related one-dimensional soft mode is located at low temperatures at the zone boundary A point of the Brillouin zone[8] (this soft mode directly condensates at this point in the pure polymer compound). If for type-I incommensurate systems incommensurability originates from the existence of a Lifschitz gradient,[35] in incommensurate systems of type-II like thiourea,[36,37] it originates from the coupling of the order parameter η (associated to the soft mode) to a secondary degree of freedom ξ transforming as η. One can more generally say that the order parameter η in pTS can be coupled at the P point ($\mathbf{q}_S=a^*/2\pm\delta b^*$) with a degree of freedom ξ, the same coupling being forbidden at the A point ($\mathbf{q}_c=a^*/2$).

The correlations between the A point and the P point are[38]

A		P
A_g, A_u	⟶	τ_1
B_g, B_u	⟶	τ_2

The star of $\mathbf{q}_S=a^*/2+\delta b^*$ contains two vectors. The dimensionality of the order parameter, which is the product of the number of vectors in the star and the number of the dimension of the small representation τ_2, is then 2.

The correlations between the A point and the Γ point are

Γ		θ		A
A_g, B_u	⟶	θ_1	⟶	A_g, B_u
B_g, A_u	⟶	θ_2	⟶	B_g, A_u

Finally, the irreducible representations of the A point in the high-temperature (HT) phase transform into the representations of the Γ point in the low-temperature (LT) commensurate phase:

A_{HT}		Γ_{LT}	
A_g	$\longrightarrow$	B_g	
B_g	$\longrightarrow$	A_g	(soft mode) .
A_u	$\longrightarrow$	B_u	
B_u	$\longrightarrow$	A_u	

These diagrams show that the order parameter has a B_g symmetry at the A point in the high-temperature phase. It can be coupled at the P point to modes having B_g or B_u symmetry at the A point. As we are looking at a degree of freedom ξ which cannot couple to η at the A point, we arrive at the conclusions that this degree of freedom has B_u symmetry at the A point and A_u or B_u symmetry at the Γ point.

Our results (Sec. IV) show that the lowest acoustic branch is the TA1 branch propagating along a^*. At the Γ point of the Brillouin zone, this A_u branch involves displacements of atoms in the b direction of incommensurability.[27] It corresponds also to the lowest frequency mode of θ_2 symmetry between the Γ point and the A point. As the soft mode has B_g symmetry at the A point and then θ_2 symmetry between the Γ point and the A point, we arrive at the conclusion that the soft mode and the TA1 mode belong to the same phonon branch. The TA2 mode located just above the TA1 mode has B_u symmetry at the Γ point and thereafter θ_1 symmetry between the Γ point and the A point. Then the TA2 mode could have B_u symmetry at the A point and then correspond to a degree of freedom ξ. The additional weak mode which was detected near $\mathbf{Q}_S$ at $T=201$ K (Sec. IV B) could be related to this TA2 mode and to the degree of freedom ξ. It is easy to understand that the situation for pTS is experimentally more complicated than for compounds like thiourea having a lock-in near the Γ point. To go beyond the results of group theory, it is necessary to have a microscopic description of all modes, particularly at the A point. Figure 12 shows the dispersion curves at $T=249$ K and Fig. 13 the dispersion curves at $T=201$ K according to our hypothesis. Similarities exist with the case of BCPS.[39,40] For this organic compound with a monoclinic structure ($I2_1/a$), incommensurability corresponds also to the condensation of a soft phonon along the zone boundary ($\mathbf{q}_s=a^*\pm\delta b^*$ for BCPS). This mode belongs to the same branch as one of the transverse acoustic phonons.

B. Influence of polymerization

The comparison of pTS-D monomer and pTS-D polymer is very interesting because this system offers, together with the other diacetylene DNP,[41,42] the only opportunity to study the influence of polymerization on a structural phase transition. In the case of DNP, a displacive transition occurs in the monocrystalline monomer[43] and not in the polymer. The disappearing of long-range ordering in the mixed monomer polymer of DNP is then easier to understand than in some orientational glasses like KBr-KCN.[44] For pTS-D, the influence of disorder in mixed monomer polymer is more subtle. We already know[8,9] that in pTS-D monomer the transition occurs almost at the same temperature ($T_i=195$ K) as for good quality pTS-D polymer monocrystal ($T_c\cong 190$ K). In both cases the analysis of x-ray thermal motions by the rigid-body method[7,8] shows that the main librational motion occurs around the same vector and is the precursor for the transition which leads to the two different positions occupied by the side groups on two inequivalent sites in the low-temperature phase. The amplitude of motion is also the same. (The incommensurability aspect is neglected in the present discussion.) We have postulated up to now that the dynamical properties of pTS-D monomer and polymer should be very different.[8,18] The result of the present study shows clearly that this hypothesis is wrong. The soft mode presents roughly the same mean-field behavior for pTS-D monomer [$\omega_c^2(0)=a(T-T_i)$, $a=7.1\times10^{-4}$ THz^2 K^{-1}, $T_i=193$ K] and pTS-D polymer[8] [$\omega_c^2(0)=a(T-T_c)$, $a'=7.3\times10^{-4}$ THz^2 K^{-1}, $T_c=190$ K].

The fact is that, even if monomer and polymer present many similarities, the signatures of the phase transition as viewed by calorimetry disappear in mixed monomer-polymer crystals of pTS-H[13,14] and pTS-D.[9] The same result is obtained by x-ray and neutron diffraction.[10,11,12] Dielectric measurements still give a weak signature[15] but it is known[44] that it could correspond only to local ordering. As pTS-D monomer and polymer have the same critical temperature T_c, the same order parameter, and the same soft mode evolution, other explanations have to be found to explain the disorder observed at intermediate polymer content. In the case of the NaCN-KCN orientational glass, local distortions of cells are due to the difference of Na^+ and K^+ radii. For pTS-D the reduction of the b parameter from the monomer (Fig. 1) ($b\cong5.16$ Å at $T=280$ K) to the polymer ($b\cong4.9$ Å at $T=280$ K)[8] is due to the substitution of van der Waals bonds by covalent bonds during polymerization. The study of the disorder that can result in mixed monomer-polymer crystals is now in progress.[45] We must point out that the situation in pTS-D is slightly different from that in NaCN-KCN glass. In addition to random strains resulting from cell distortions, Blinc[46] pointed out that in NaCN-KCN random bonds may not be neglected. The large difference in critical temperature for pure NaCN and KCN[44] illustrates this effect. pTS-D is then probably a better prototype of the pure random field case.[47] The question is now to know whether or not this random field is sufficiently strong to suppress the phase transition in mixed crystals. A study by neutron scattering is in progress to check this point, together with the specific effect related to the extended character of the defects (polymer chains).[45]

ACKNOWLEDGMENTS

We thank C. Ecolivet (Groupe Matiére Condensée et Matériaux), B. Hennion, and P. Bourges (Laboratoire Léon Brillouin) for useful discussions. The Groupe Matière Condensée et Matériaux is "Unité de Recherche Associée au C.N.R.S. No. 804."

[1]G. Wegner, Z. Naturforsch. **24b**, 824 (1969).
[2]M. Bertault, thesis, University Paris VII, 1983.
[3]P. Robin, J. P. Pouget, R. Comes, and A. Moradpour, J. Phys. (Paris) **41**, 415 (1980).
[4]Van D. Kobelt and E. F. Paulus, Acta Crystallogr. B **30**, 232 (1974).
[5]V. Enkelmann, Acta Crystallogr. B **33**, 2842 (1977).
[6]V. Enkelmann and G. Wegner, Makromol. Chem. **178**, 635 (1977).
[7]J. P. Aime, J. Lefebvre, M. Bertault, M. Schott, and J. O. Williams, J. Phys. (Paris) **43**, 307 (1982).
[8]J. Even, M. Bertault, B. Toudic, H. Cailleau, J. L. Fave, R. Currat, and F. Moussa, Phys. Rev. B **49**, 11 602 (1994).
[9]J. Even, thesis, University Paris VI, 1992.
[10]J. N. Patillon, P. Robin, P. A. Albouy, J. P. Pouget, and R. Comes, Mol. Cryst. Liq. Cryst. **76**, 297 (1981).
[11]J. P. Aime, thesis, University Paris VII, 1983.
[12]J. P. Aime, M. Bara, M. Bertault, and M. Schott, Mater. Sci. **10**, 441 (1984).
[13]I. Hatta, T. Nakayama, and T. Matsuda, Phys. Status Solidi B **62**, 243 (1980).
[14]M. Bertault, A. Collet, and M. Schott, J. Phys. Lett. **42**, I **131** (1981).
[15]R. Nowak, J. Sworakowski, B. Kuchta, M. Bertault, M. Schott, R. Jakubas, and H. A. Kolodziej, Chem. Phys. **104**, 467 (1986).
[16]M. Bertault, M. Krauzmann, M. Le Postollec, R. M. Pick, and M. Schott, J. Phys. (Paris) **43**, 755 (1982).
[17]J. Even, M. Bertault, B. Toudic, H. Cailleau, F. Moussa, A. Girard, and Y. Delugeard (unpublished).
[18]J. Even, H. Cailleau, B. Toudic, M. Bertault, F. Moussa, and R. Currat, Physica B **180**, 339 (1992).
[19]V. Enkelmann, R. J. Leyrer, and G. Wegner, Makromol. Chem. **180**, 1787 (1979).
[20]M. Bertault, M. Schott, M. J. Brienne, and A. Collet, Chem. Phys. **85**, 481 (1984).
[21]H. Grimm, D. Axe, and C. Krohnke, Phys. Rev. B **25**, 1709 (1982).
[22]M. Hennion, F. Hippert, and A. P. Murani, J. Phys. F **14**, 489 (1984) (Appendix).
[23]B. Dorner, in *Coherent Inelastic Neutron Scattering in Lattice Dynamics,* Vol. 93 of *Springer Tracts in Modern Physics,* edited by G. Höhler (Springer-Verlag, Berlin, 1982).
[24]R. Currat and T. Janssen, Solid State Phys. **41**, 201 (1988).
[25]M. Quilichini and R. Currat, Solid State Phys. **48**, 1011 (1983).
[26]R. Leyrer, G. Wegner, and W. Wettling, Ber. Bunsenges, Phys. Chem. **82**, 697 (1978).
[27]W. Rehwald, A. Vonlanthen, and W. Meyer, Phys. Status Solidi **75**, 219 (1983).
[28]J. P. Aime (unpublished results).
[29]B. Dorner and R. Comes, in *Dynamics of Solids and Liquids by Neutron Scattering,* Vol. 3 of *Topics in Current Physics,* edited by S. W. Lovesey and T. Springer (Springer-Verlag, Berlin, 1977).
[30]B. I. Halperin and C. M. Varma, Phys. Rev. B **14**, 4030 (1976).
[31]A. P. Levanyuk and A. S. Sigov, in *Defects and Structural Phase Transitions,* Vol. 6 of *Ferroelectricity and Related Phenomena* (Gordon and Breach, New York, 1988).
[32]V. A. Golovko an A. P. Levanyuk, in *Light Scattering Near Phase Transitions,* edited by H. Z. Cummins and A. P. Levanyuk (North-Holland, Amsterdam, 1983), p. 169.
[33]D. Durand, F. Denoyer, R. Currat, and M. Lambert, in *Incommensurate Phases in Dielectrics-Materials,* edited by R. Blinc and A. P. Levanyuk (North-Holland, Amsterdam, 1986), p. 101.
[34]F. Denoyer and R. Currat, in *Incommensurate Phases in Dielectrics-Materials,* edited by R. Blinc and A. P. Levanyuk (North-Holland, Amsterdam, 1986), p. 129.
[35]A. P. Levanyuk and D. G. Sannikov, Sov. Phys. Solid State **18**, 1126 (1976).
[36]A. P. Levanyuk and D. G. Sannikov, Sov. Phys. Solid State **18**, 1122 (1976).
[37]I. Aramburu, G. Madariaga, and J. P. Perez-Mato, Phys. Rev. B **49**, 802 (1994).
[38]J. Zak, A. Casher, M. Gluck, and Y. Gur, in *The Irreducible Representations of Space Groups* (Benjamin, New York, 1969).
[39]K. Saito, K. Kikuchi, and I. Ikemoto, Solid State Commun. **81**, 241 (1992).
[40]J. Etrillard, J. Even, M. Sougoti, P. Launois, S. Longeville, and B. Toudic, Solid State Commun. **87**, 47 (1993).
[41]G. Nemec and E. Dormann, J. Phys. Condens. Matter **4**, 5599 (1992).
[42]H. Winter, E. Dormann, M. Bertault, and L. Toupet, Phys. Rev. B **46**, 8057 (1992).
[43]J. Even, M. Bertault, A. Girard, Y. Delugeard, and J. L. Fave, Chem. Phys. **188**, 235 (1994).
[44]U. T. Hochli, K. Knorr, and A. Loidl, Adv. Phys. **39**, 5 (1990).
[45]S. Longeville, M. Bertault, J. Even, and F. Moussa (unpublished).
[46]R. Blinc, Z. Naturforsch. **45A**, 313 (1990).
[47]J. P. Pouget, Europhys. Lett. **11**, 645 (1990).